Hawassa University Journals - Ethiopia
Ethiopian Journal of Engineering and Technology (EJET)
Volume 5, 2026, Pages 43 – 64. https://doi.org/10.82127/ejet.v5i1.2154

Mechanical and Microstructural Performance of Concrete Incorporating River and Quarry Sand

Zelealem Mekonnen[1], Fiseha Sahile[2] & Tariku Nigussie[3,*]

[1]*Department of Civil Engineering, Institute of Technology, Hawassa University, Hawassa, Ethiopia.*

[2]*Facultyt of Civil Engineering, Arba Minch Institute of Technology, Arba Minch, Ethiopia.*

[3]*Department of Construction Technology and Management, Institute of Technology, Hawassa University, Hawassa, Ethiopia.*

Corresponding Author: Tariku Nigussie (tarikun@hu.edu.et)

Abstract

The increasing scarcity of natural river sand and the environmental impacts associated with its extraction necessitate systematic evaluation of alternative fine aggregates for sustainable concrete production. This study investigates the mechanical and microstructural performance of concrete incorporating river and quarry sands sourced from eight locations around Hawassa City, Ethiopia. Four river sands and four quarry sands were characterized for physical, chemical, and mineralogical properties in accordance with ASTM and Ethiopian standards. Concrete mixtures were proportioned using a constant water–cement ratio of 0.50 and a nominal mix ratio of 1:1.5:2.6, targeting a 28-day compressive strength of 33.5 MPa. Fresh concrete exhibited comparable workability, with slump values ranging from 76 to 82.5 mm and compaction factors between 0.816 and 0.853. At 28 days, compressive strength varied from 23.14 to 33.86 MPa, while splitting tensile strength ranged from 11.98 to 15.01 MPa. Water absorption results indicated lower permeability for concretes produced with well-graded sands. Scanning Electron Microscopy revealed pore area values between 17.96 % and 28.56 %, demonstrating a strong inverse relationship with compressive strength. X-ray Diffraction confirmed quartz as the dominant mineral phase influencing hydration behavior. The findings demonstrate that properly processed

quarry sand can achieve mechanical and microstructural performance comparable to river sand when stringent quality control measures are applied.

Keywords: Fine Aggregate; Quarry Sand; River Sand; Concrete Strength; Microstructure; SEM; XRD

1. Introduction

Concrete is indeed the most common building material used all over the world. This is because concrete can be made from readily available materials, it is durable, and it can be used for a wide range of structural works. Concrete is mostly made up of aggregates, which make up about 65- 75% of the whole concrete. And among these aggregates, fine aggregates are the key factors that determine workability, strength, durability, and even performance over time (Mehta & Monteiro, 2014; Neville, 2011). For a long time, natural river sand was used as the fine aggregate of choice; however, the excessive extraction has led to environmental degradation, depletion of riverbeds, and stricter regulations. These problems have made it even more urgent to find alternatives that are not only technically reliable but also environmentally friendly (Kumar & Ransinchung, 2023).

The by-product of the rock crushing activities is the production of quarry sand, which has become one of the possible replacements for the natural river sand in most regions. Earlier experiments have proven that concrete made of quarry sand that has been processed properly can reach similar or even higher mechanical properties when the issues of grading, cleanliness, and moisture are addressed (Ali et al., 2023; Siddique & Singh, 2022). What occurs within the mix, however, is directly related to what sort of minerals the original rock consists of, the degree to which the grains are jagged or rounded, or the amount of undesired dust or clay is leached through (Aslani et al., 2020). Since the crust of the earth moves a lot between zones, what we may observe at one place may not be repeated in our locality, where the underground layers will turn in a different direction.

The city is quickly becoming urbanized in Ethiopia, and the infrastructure is being built at a rapid rate, thus raising the demand for construction materials. There are a number of river and quarry sand sources around Hawassa City that are currently utilized in the construction of structural concrete. Although widely used, material selection is commonly not performed in line with scientifically proven performance, but with available materials. The lack of systematic, place-specific research assessing the mechanical and microstructural performance of concrete produced using such locally sourced sands brings an element of uncertainty in the quality management and imposes possible threats to the structural serviceable life and durability (Kebede et al., 2022).

Recent developments in the concrete research focus indicate that the mechanical performance cannot be completely used to describe material behavior. Microstructural features including pore structure, hydration products distribution and the nature of interfacial transition zone (ITZ) would be critical in the control of strength, permeability, cracking resistance and durability (Bentz et al., 2017). The Scanning Electron Microscopy (SEM) and X-ray Diffraction

(XRD) methods are useful in clarifying these micro-level processes, which can be used to obtain a more detailed idea of how aggregate properties affect concrete performance (Zhao et al., 2023). The mineralogical composition, crystallinity and angularity of particles may cause large discrepancies in hydration efficiency and densification of the matrix, despite holding the nominal mix proportions constant (Singh et al., 2024).

It is stated that a large silt and clay content, increased water absorption, and organic impurities in fine aggregates negatively influence the concrete strength and durability (Domagała, 2015; Raja & Vijayan, 2020). On the other hand, graded sands with good mineralogical make-up increase the particle packing, reduce the porosity and enhance load transfer within the cementitious mass (Elat et al., 2020). Nevertheless, the majority of current research is dedicated to general comparison of river and crushed sands, and minimal consideration is paid to material variability in regions and combined mechanical-microstructural analysis.

Such combined studies are not common in the Hawassa and surrounding regions. The local geological diversity indicates that sands found in dissimilar rivers and quarries could have significant differences in the physical, chemical, and mineralogical characteristics, which subsequently affect the behavior of concrete. In the absence of empirical data, engineers and decision-makers are not in a position to make the right choice of fine aggregates to use in structural application to achieve the correct performance, price, and environmental sustainability.

Hence, the current research paper will be an in-depth comparative analysis of the concrete that has been made by using river and quarry sands collected in various places near Hawassa City, Ethiopia. The study is a combination of physicochemical characterization of fine aggregates, mechanical testing, and microstructural analysis of hardened concrete. SEM and XRD investigations are added to standard tests of strength in order to make some correlations between aggregate properties, microstructural characteristics, and macroscopic performance. The results should serve as region-representative scientific data to the overall discussion of sustainable aggregate utilization and as well as in making informed judgments towards tangible construction practice.

2. Materials and Methods

2.1. Study Area and Material Sampling

The experimental software was implemented with fine aggregates that were obtained in the regions of Hawassa City and its surroundings in Ethiopia. Sand sources that were studied included eight sand sources which included four river sand and four quarry sand. Each source was sampled to obtain approximately 150 kg of sand to comply with ASTM D75 / D75M protocols (ASTM International, 2014). The samples were allowed to dry under air over a period of 48 hrs, after which they were homogenized through the coning and quartering technique, before being subject to testing. The Monopol Quarry was used to obtain crushed coarse aggregate that had a nominal maximum size of 20 mm. The material used in the course of the study was ordinary Portland Cement (OPC) 42.5N grade that met the Ethiopian Standard ES C.D6:(2012) and was similar to

ASTM C150 (2022c) Type I. Both mixing and curing were done using potable water that fulfilled the chemical requirements of ASTM C1602 (ASTM International, 2021b).

2.2. Characterization of Aggregates

Physical and chemical characteristics of fine and coarse aggregates were measured based on the known ASTM, AASHTO, IS and BS standards. The bulk density and specific gravity were measured by ASTM C29(2018), ASTM C128(2020b) (fine aggregate), and ASTM C127(2020a) (coarse aggregate): The sieve analysis was used to determine the particle size distribution. The moisture content was determined based on ASTM C566 (2023c).

Table 1. Fine and coarse aggregate tests with standards and objectives

No.	Test	Standard	Objective
1	Sieve analysis	ASTM C33 (2023a)	Determine particle size distribution
2	Bulk density	ASTM C29 (2018)	Assess packing characteristics and void ratio
3	Specific gravity (Fine)	ASTM C128 (2020b)	Determine particle density and absorption of fine aggregates
4	Specific gravity (Coarse)	ASTM C127 (2020a)	Determine particle density and absorption of coarse aggregates
5	Moisture content	ASTM C566 (2023c)	Evaluate moisture condition prior to mixing
6	Silt content	IS 2386 (1963a, p. 23)	Identify clay and silt fines that can affect bonding
7	Clay content	ASTM C33-93 (2023a)	Ensure clay levels are within acceptable limits
8	Organic impurities	ASTM C40 (2022a)	Detect deleterious organics using NaOH colorimetric method
9	Soundness (Durability)	ASTM C88 / AASHTO T104 (2019b; 2021a)	Simulate sulfate resistance and weathering effects
10	Flakiness Index (Coarse)	IS 2386 Part I (1963a)	Assess particle shape for mix uniformity
11	Aggregate Impact Value	IS 2386 Part IV (1963b)	Determine aggregate resistance to sudden impact
12	Aggregate Crushing Value	BS 812 (1990)	Assess mechanical strength under compressive load
13	Los Angeles Abrasion	AASHTO T96 (2019a)	Evaluate resistance to abrasion/wear

The contents of silt and clay were determined by utilizing IS 2386(1963a) (Part I), whereas the contents of organic impurities were determined by the colorimetric method, which was defined in ASTM C40 (2022a). Soundness tests were considered as an indicator of aggregate durability by administering sodium sulfate as per ASTM C88 (2021a) and AASHTO T104 (2019b). Aggregate impact value (IS 2386 Part IV(1963a)), aggregate crushing value (BS 812 Part 110 (1990)) and Los Angeles abrasion tests (AASHTO T96 (2019a)) were used to determine the mechanical resistance of coarse aggregates. Table 1 summarizes the tests and their respective standards chosen.

2.3. Concrete Mix Design and Specimen Preparation

The proportions of the concrete mix were based on the ACI 211.1, aiming to the compressive strength at 28 days -33.5 MPa (C-25 grade) (American Concrete Institute (ACI), 2009). The ratio of water to cement was kept constant at 0.50 to eliminate the effect of the variability of the sand sources. The estimated nominal mix ratio of weight was 1: 1.5: 2.6 (cement fine aggregate: coarse aggregate), and no chemical admixtures were added. Each of the tests was cast in concrete specimens in triplicate. Cubes of 150 mm x 150 mm x 150 mm were prepared to go through compressive strength, rebound hammer and water absorption tests and cylinders of 150 mm x 300 mm were used to carry out splitting tensile strength tests. Further samples were casted to microstructure. Demolding and water-curing after 24 hrs, all specimens were demolded and water-cured at temperature $20 \pm 2\ ^{0}C$ until the required testing ages had been attained.

2.4. Testing of Fresh and Hardened Concrete

Fresh concrete workability was evaluated using the slump test (ASTM International, 2022b) and the compaction factor test (ASTM C403) (2023b). Hardened concrete properties were assessed at 7 and 28 days. Compressive strength tests were performed according to ASTM C39, and splitting tensile strength was determined following ASTM C496. Surface hardness and in-place strength estimation were evaluated using the rebound hammer test in accordance with ASTM C805 (2022d). Water absorption was measured following BS 1881-122 to assess concrete permeability characteristics.

2.5. Microstructural Analysis

Scanning Electron Microscopy (SEM) and X-ray Diffraction (XRD) were used to microstructure characterize chosen aggregate samples and 28-day concrete samples. Morphology of the surface, pore structure, and interfacial transition zone (ITZ) were studied with a microscope, JEOL JSM-IT300, to perform SEM. To compare porosity and particle morphology with SEM images, ImageJ software was employed to analyze images in accordance with the guidelines of image-based analysis (Bentz et al., 2017). To determine crystalline phases and determine mineralogical composition of natural sands and hardened concrete, XRD analysis was done. Cu Ka radiation patterns were recorded in a range of 10°-80° 2θ . Sizing of crystallites was measured by the Scherrer equation whereas the spacing between the interplanar was by the Bragg equation

(Bragg & Bragg, 1913; Scherrer, 1918). The representative XRD and SEM results are discussed in the Figures 2-9 and 10-25, respectively.

2.6. Data Analysis

Micro-characterization of the chosen aggregate samples and 28-day concrete specimens was conducted according to the Scanning. All test results are presented in the form of average values, which were obtained in triplicate specimens. Comparison analysis was conducted in order to compare the differences between river sand and quarry sand concrete. The correlation of aggregate properties, microstructural properties, and mechanical performance was studied to detect the controlling trends and performance-regulating parameters.

3. Results and Discussion

3.1. Properties of Aggregates and Compliance with Standards

The physical and chemical characteristics of the fine aggregates studied had significant differences based on the source, which was due to the heterogeneous geology in the area of Hawassa City. The sands of rivers and quarry met major requirements of ASTM C33 (2023a) and Ethiopian standards, but some of them were beyond the limits of the silt and clay content, water absorption, and organic impurities. Quarry sands tended to be more angular and rough-surfaced but river sands had a smoother morphology of their particles. Sands with high fines and organic content, especially the ones obtained in Ayermarefiya and Shamena, had lower unit weight, and increased the values of bulking, suggesting poor packing behavior. It is known that these deficiencies elevate the water demand and change the cement hydration process, which, in turn, negatively affects the development of concrete strength (Domagała, 2015; Raja & Vijayan, 2020). Conversely, Hantate River and Langano Quarry sands showed good grading and specific gravity which implied better particle packing and transfer of loads.

3.2. Fresh Concrete Properties

Fresh concrete the workability was measured on the basis of the slump and compaction factor tests; those values were within the range of target values across all mixes. The average result of slump test at each location was as follows: Aje(Bura) quarry 76 mm; Ayermaref iya quarry 82.5mm, Blate River 81mm, Dimitu river 80mm, Hantate River 80mm, Langano quarry 79mm, Shamena quarry 77.5mm and Weterarares a river 80.5mm. The fact that there is minimal differences in the values of slump with the various sources of sand implies that the workability was reduced at the fresh state by maintaining the same water-cement ratio. The compaction factor registered a maximum of 0.853 on Ayermarefiya quarry mix and a minimum of 0.816 on the Dimitu river mix. The factors of all the other sources (Aje(Bura) quarry, Blate River, Hantate River, Langano quarry and Weterararesa river) were between 0.830 and 0.845. Nevertheless this seeming homogeneity does not suggest similar rigorous performance since new concrete tests are less susceptible to fines content and micro-structural shortcomings (Neville, 2011).

3.3. Compressive Strength Development

The compressive strength results revealed clear performance differentiation between concrete mixes prepared with different sand sources (Table 2).

Table 2. Compressive Strength Test Result

Sample Names	Average Compressive Strength Test Result						Strength relationship (%)	
	7th Day		28th Day		Designed			
	(Mpa)	Std. ±	(Mpa)	Std. ±	7th Day	28th Days	7th Day	28th Day
Hantate River	30.51	3.91	33.33	4.08	21.78	33.5	91.1	99.5
Aje (Bura) Quarry	20.94	3.24	29.51	3.82			62.5	88.1
Ayermarefya Quarry	17.95	3	23.14	3.4			53.6	69.1
Blate River	31.79	3.99	33.59	4.1			94.9	100.3
Dimitu River	27.56	3.71	31.20	3.95			82.3	101.1
Langano Quarry	28.63	3.78	33.86	4.11			85.5	101.1
Shamena Quarry	24.49	3.90	29.67	3.84			75.5	86.2
Weteraresa River	25.29	3.56	28.86	3.8			73.1	88.6

River sand concretes tended to have better 7- and 28-day strengths than quarry sand concretes, with some significant exceptions. The concrete made using Hantate River and Langano Quarry sands met or surpassed the target 28-day compressive strength of 33.5 MPa, showing that quarry sands can be just as useful in the case when the quality of the materials is sufficient.

On the other hand, concrete that used Ayermarefiya Quarry sand could not fulfill the requirements of strength on all ages of curing. This poor performance has been reported to be caused by high water absorption level, high fines, and low specific gravity which all contributed to weakening cement-aggregate bond and made it more porous. The same tendencies (although with less significance) were observed in the case of Shamena Quarry and Weteraresa River sands. The current results, coinciding with the prior works that indicated high clay content and low

grading substantially lowered compressive strength (Elat et al., 2020; Siddique & Singh, 2022), would have been expected in this case. The values of standard deviation showed that the strength variation of concretes manufactured using marginal-quality sands was higher, which implies that the hydration was not always uniform and the matrix had local weak points. This variability evokes the questions of structural reliability and emphasizes the importance of severe control of material quality.

3.4. Rebound Hammer and Tensile Strength Performance

The results of the rebound hammer test were in the same direction with the compressive strength results (Table 3). Good quality of concretes, including the ones that had been made using Hantate River and Blate River sands, had a higher rebound number resulting in an increase in surface hardness and uniformity. Reduced values of rebound observed in quarry sand concretes that are found to have high content of impurity indicate weaker surface areas and poor cement paste quality (ASTM International, 2022b).

Table 3. Rebounded Hammer test result

Sample Name	**Corresponding Rebound average 28th Days**	**SD**	**Quality of concrete**	**Pont Position**
Hantate River	33.4	4.08	Good Layer	CUBE (Hor.→)
Aja (Bura) Quarry	26.3	3.82	Fair	
Ayermarefiya Quarry	26.1	3.4	Fair	
Blate River	32	4.1	Good Layer	
Dimtu River	30.35	3.95	Good Layer	
Langano Quarry	28.5	4.11	Fair	
Shemena Quarry	25.7	3.84	Fair	
Weteraresa River	27.6	3.8	Fair	

The tensile strength division acted as the additional confirmation of the impact of sand source on concrete performance (Table 4). Well-graded sands in concretes showed better tensile resistance, as it showed better stress transfer across the interfacial transition zone (ITZ). Combines with low grade or highly absorptive sands were less tensile strong, more prone to crackage and failures due to durability.

Table 4. Tensile Splitting Test Result

Cube Id / Sample Name	Types of Specimens	Average Compressive Strength (Mpa)	
		7th	28th
Hantate river	15mm × 300 mm Dimensions Cylinder	12.458	14.689
Aje (Bura) quarry		10.362	13.043
Ayermarefiya quarry		9.644	12.743
Blate river		11.087	14.262
Dimitu river		12.429	15.005
Langano quarry		11.887	14.944
Shamena quarry		9.324	11.978
Weteraresa quarry		10.934	13.760

3.5. Water Absorption and Durability Implications

The absorption of water in the tested concretes gave varying outcomes. The values of absorption were higher in mixes that were prepared using high fines and porous sands, which showed high permeability but low durability (Figure 1). Increased water uptake is frequently linked to interrelated pore networks that allow the influx of moisture and the faster rate of deterioration processes (Mehta & Monteiro, 2014). Hantate River and Langano Quarry sands were used to prepare concretes which showed relatively lower absorption due to denser microstructures and better hydration. The findings imply a higher potential of long-term durability, especially where the environment is hostile.

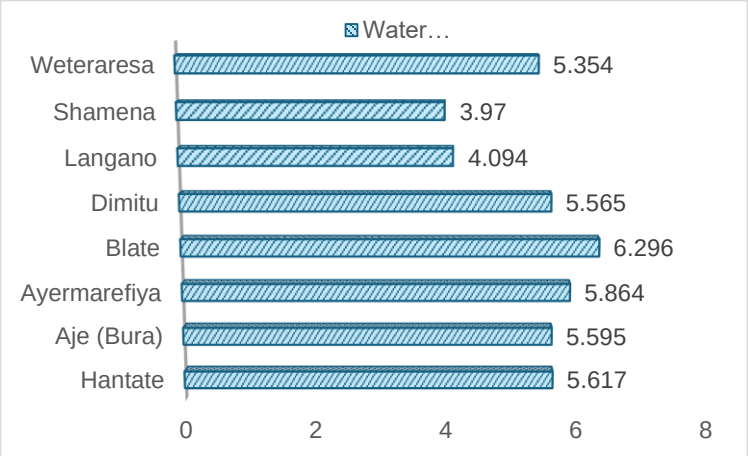

Figure 1. Water Absorption of Concrete

3.6. Microstructural Characteristics (SEM and XRD)

3.6.1. X-ray Diffraction Analysis

XRD revealed quartz (SiO_2) as the main crystalline phase of both natural sands and hardened concretes with small differences in the position and intensity of peaks by the sand source (Fguer 2-9). Crystallinity and peak broadening differences are indications of mineral purity and crystallite size. Prepared concretes that contained better sands had sharper hydration-related peaks, which means that the formation of the calcium silicate hydrate (C-S-H) phases were more effective. Remarkably, sands with secondary peaks that were related to accessory minerals, e.g. calcite were related to concretes with modified hydration characteristics and diminished strength. These conclusions are feasible in light of the reports that associated mineralogical impurities with impaired cement hydration and diminished strength (Zhao et al., 2023).

Aje (Bura) quarry sands 28th concrete the XRD pattern showed a peak at 2θ = 34.197° with a D-spacing of 2.6199 Å and a peak width of 0.541° (Figure 2). Aje (Bura) Quarry Sands 28th days Concrete has a higher 2θ angle and narrower peak, possibly indicating a more crystalline material compared to Aje (Bura) Quarry Natural Sands. Aje(Bura) Quarry Sand Concrete: Exhibits a notable cluster around 29.66922^0 and 30.99403^0, and a very sharp peak at 47.30946^0. The peaks for the cement hydration products are exceptionally strong relative to the quartz peak. Specifically, the Portlandite peak at 18.05627^0 (≈190 au) and the C-S-H peak at 34.24^0 (≈240 au) are highly prominent. This may imply a comparatively higher cement content or a very efficient hydration reaction in this mix.

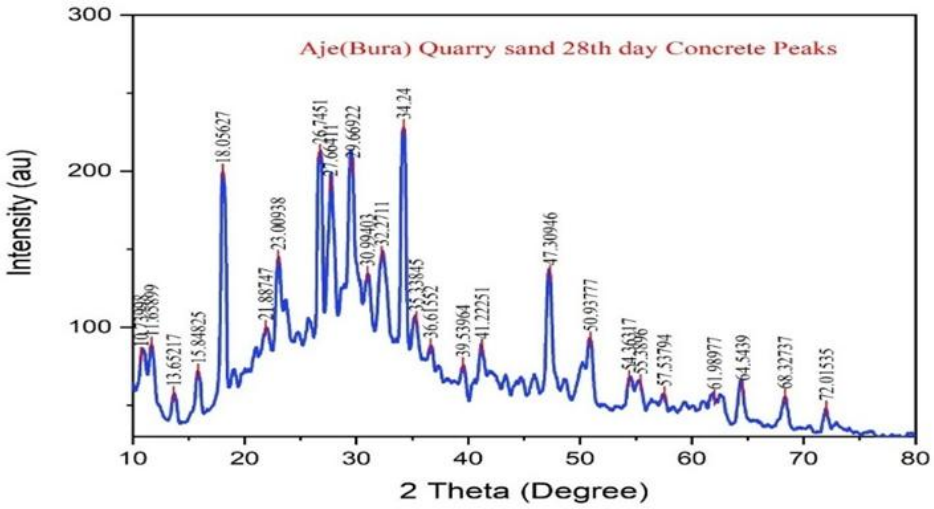

Figure 2. Aje (Bura) quarry sand 28th concrete Peak analysis result

Ayermarefiya quarry sands 28th concrete the XRD pattern showed a peak at 2θ = 27.6° with a D-spacing of 3.2204Å and a peak width of 0.5729° (Figure 3). The XRD patterns of the two samples are quite similar, with minor differences in peak position and peak width. Ayermarefiya Quarry Sand Concrete: Has a noticeable peak at 29.40665^0 and a clear distinction between the peaks at 17.99659^0 and 21.68457^0 exhibits a clear, strong shoulder peak at 29.40665^0 (≈240 au),

similar to Weterarisa, suggesting a notable accessory mineral content (likely Calcite or another crystalline impurity) in the quarry sand.

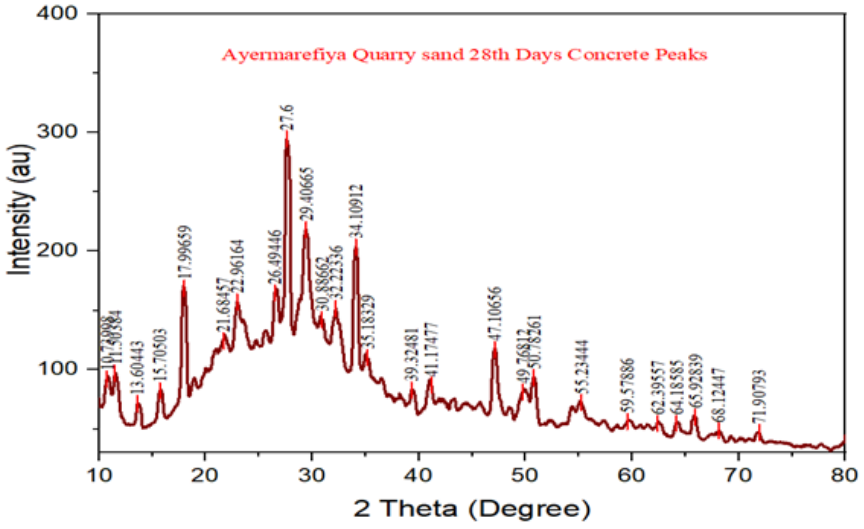

Figure 3. Ayermarefiya quarry sand 28th concrete Peak analysis result

Blate River sands 28th concrete XRD pattern revealed a peak at $2\theta = 26.72^0$ having a 3.3364 A D-spacing and a width of the peak was 0.569^0 (Figure 4). The XRD pattern of the two samples is rather similar with slight differences in the position and the width of the peaks. Shows a clear, resolved, well-separated spectrum, with a strong hydration peak at 34.18^0. The 2θ value of the main peak is slightly smaller than the mean 27.6^0, indicating that there is a slight difference in the lattice parameters of the quartz of this particular river source.

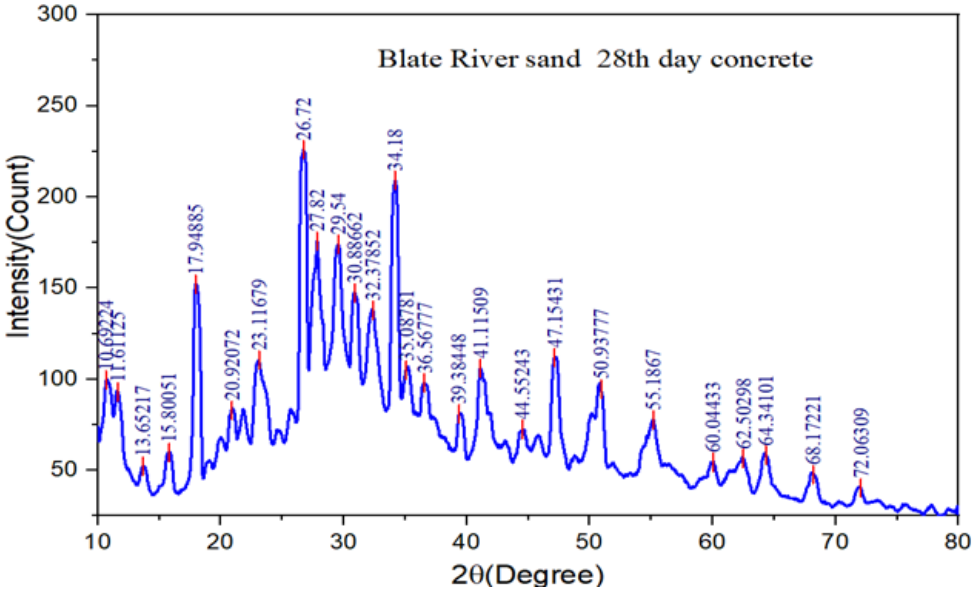

Figure 4. Blate River sand 28th concrete Peak analysis result

Sands of Dimtu river 28th days concrete XRD pattern revealed a peak at 2θ =27.76^0 with D spacing=3.2055 A peak width=0.571^0(Figure 5). The XRD spectrums of the two samples are relatively close with slight variations on the position of peaks and the width of the peaks. Dimtu River Sand Concrete: Has a clear sharp peak at 36.64^0 which is not as high in most other samples. The highest value of 70.4757^0 is also not very weak. There is a sharp peak that is noticeable at 36.64^0, which is not as prominent in other samples, which may indicate a certain content of accessory minerals.

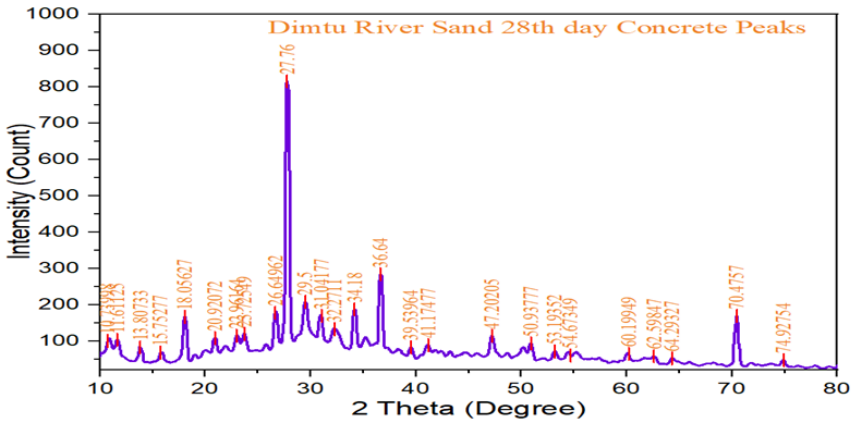

Figure 5. Dimtu River sand 28th concrete Peak analysis result

The XRD pattern of the hantate river sands 28th concrete indicated a peak at 2θ = 27.68^0 with a D-spacing of 3.2089A and a peak width of 0.586^0(Figure 6). The XRD profiles of the two samples are rather similar with slight variations in the peak position and the width of the peak. Hantate River Sand Concrete: There is a very sharp peak of 41.86(≈430 counts). That is very noticeable. Although there are other samples with a peak around this area, its eminence in Hantate indicates a sizable amount of yet another crystalline form perhaps another silicate or perhaps an impurity mineral. The sample is peculiar as there is a very strong secondary peak at 41.86^0 (≈430 counts).

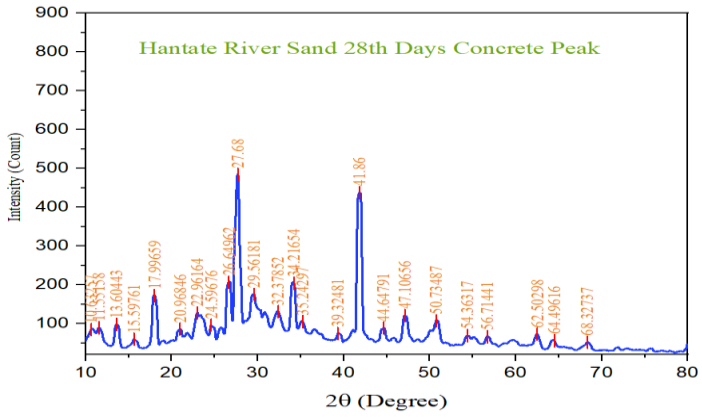

Figure 6. Hantate river sand 28th concrete Peak analysis result

This is a high intensity of 41.86^0 which indicates that there is a considerable percentage of one of the secondary silicate minerals or a different crystalline component characteristic of the Hantate sand. Langano quarry sands 28th concrete the XRD pattern showed a peak at $2\theta = 26.64°$ with a D-spacing of 3.3436 Å and a peak width of 0.55°(Figure 7). The XRD patterns of these two samples are quite similar with minor differences in peak position and peak width. The primary feature is a broad, strong double-peak structure composed of 26.64^0 and 27.66^0 peaks, which implies either two slightly different crystalline quartz forms or an intergrowth with another phase.

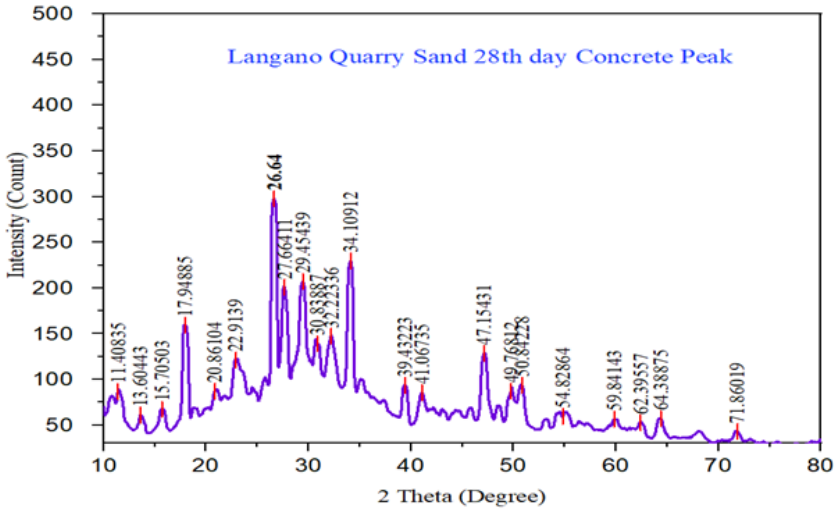

Figure 7. Langano quarry sand 28th concrete Peak analysis result

Shamena quarry sands 28th concrete the XRD pattern showed a peak at $2\theta = 27.64°$ with a D-spacing of 3.2107 Å and a peak width of 0.6°(Figure 7). The X-ray Diffraction (XRD) patterns of Shamena Quarry natural sands and Shamena Quarr Displays well-defined and multiple peaks in the hydration region (e.g., 18.104^0 for Portlandite and a prominent peak at 49.971^0), indicating a typical and successful cement hydration profiley sands in the 28th days concrete show similarities with some minor differences.

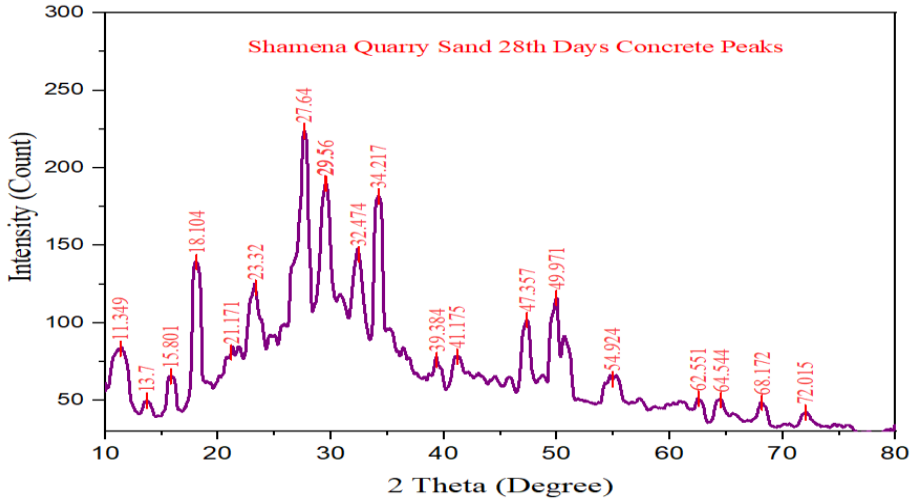

Figure 8. Shamena quarry sand 28th concrete Peak analysis result

Weteraresa river sands 28th concrete the XRD pattern showed a peak at 2θ = 27.74° with a D-spacing of 3.2852 Å and a peak width of 0.507° The XRD patterns of the two samples are quite similar, but there are some minor differences in peak position, D-spacing, and peak width. Weterarisa River Sand Concrete Shows a pronounced peak at 29.42^0 and a strong peak at 47.262^0 and 50.866^0(Figure 8). Characterized by a very strong secondary peak at 29.42^0 (≈240 counts), which is very close in intensity to the main quartz peak. This likely suggests a significant presence of a common sand impurity such as Calcite ($CaCO_3$).

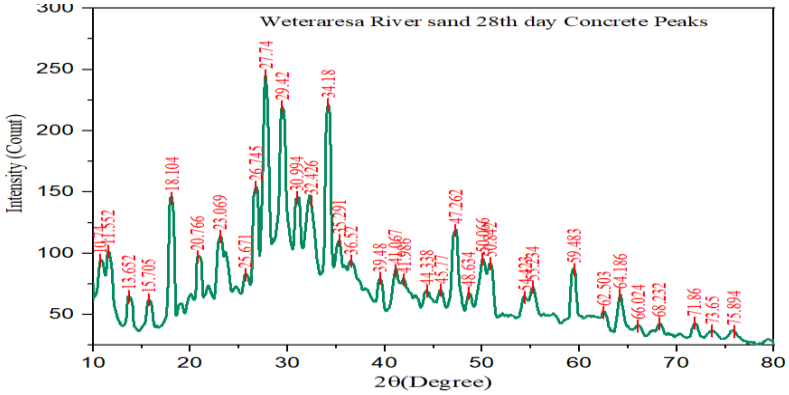

Figure 9. Weteraresa river sand 28th concrete Peak analysis result

3.6.2. SEM Analysis and Porosity - Scanning Electron Microscopy (SEM) of Concrete

Microstructure SEM test is an electron beam magnification test which is used to magnify sample on which surface features and material properties are measured. It assists in the establishment of structural parameters and is normally done with optical or scanning electron microscopes. Further size and quantity of features are quantified and measured. SEM is an effective surface analysis method at high magnifications, especially in sand analysis, the study was carried out on the formation of the concrete products in eight mix proportions with regard to sand source mixes and the relationship between the products and normal mixes.

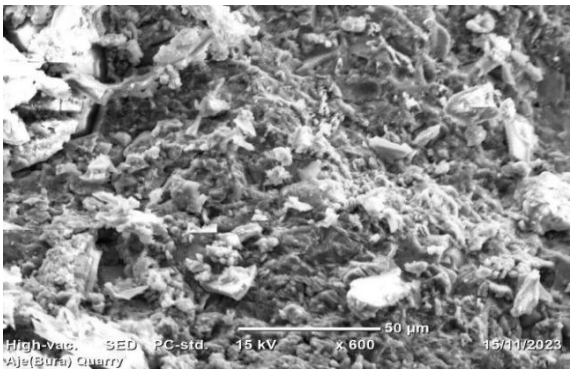

Figure 10. SEM Aje (Bura) quarry 28th day Concrete

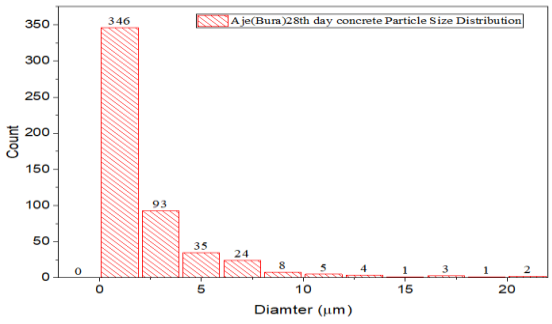

Figure 11. Aje (Bura) quarry 28th day Concrete PSD

This discussion contributes to the explanation of the strength of concrete products. SEM analysis gives in depth the information about the grain size and helps the researchers to get a clue about the material composition and possible application.

The Particle Size Distribution (PSD) graph and the Scanning Electron Microscope (SEM) image inform about the state of 28-day concrete. According to the SEM image, there is a porous and fissured appearance with a big air space, which can deteriorate the concrete and jeopardize the meeting of the requirements in terms of density, strength, and permeability. A fine cement paste is observed in the PSD graph, and this ought to assist in the hydration but is lost in the porosity that is witnessed. In general, the strength of the concrete is doubtful regarding its future application in building. The results of the analysis of the SEM image and Particle Size Distribution of the 28-day concrete of the Aje (Bura) quarry reveal that the microstructure is strong and dense. The SEM picture shows that it has a small matrix with hydration products such as Calcium Silicate Hydrate, which implies low porosity. Very fine size of particles facilitates their easy packing and few coarse cement particles are present.

The analysis reveals a rough, porous microstructure with voids from a 28-day cure, primarily composed of very fine particles (≈80% <10 μm). This fine material aids micro-void filling, but SEM images show imperfections leading to residual porosity and an irregular matrix structure.

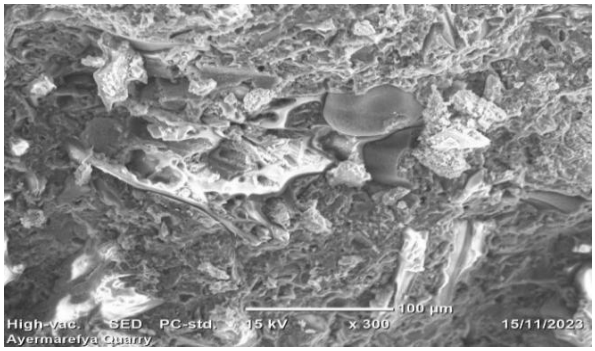

Figure 12. SEM Ayermarefiya quarry 28th day Concrete

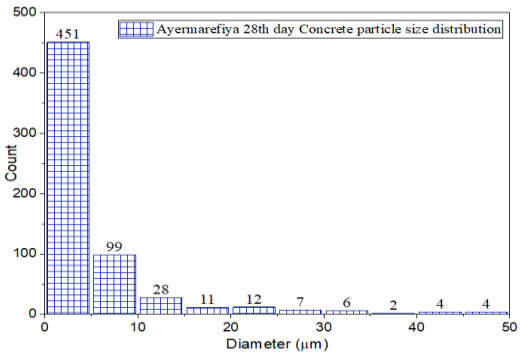

Figure 13. Ayermarefiya quarry 28th day Concrete PSD

The Blate River sand concrete has a microstructure built from excellent ultrafine components, but the resulting matrix shows critical structural defects (micro cracks), likely stemming from the poor overall gradation of the combined materials leading to shrinkage stresses.

The Dimtu River sand concrete exhibits a microstructure characterized by a highly dense, well-hydrated, and low-porosity matrix. The absence of major microcracks suggests good structural integrity and potentially high compressive strength.

The Hantate River sand concrete exhibits a notably rough surface (Figure 18) and is characterized by the highest concentration of ultrafine particles (698 counts in 0-2 μm diameter, Figure 19), suggesting a matrix rich in cement hydration products and/or very fine sand dust

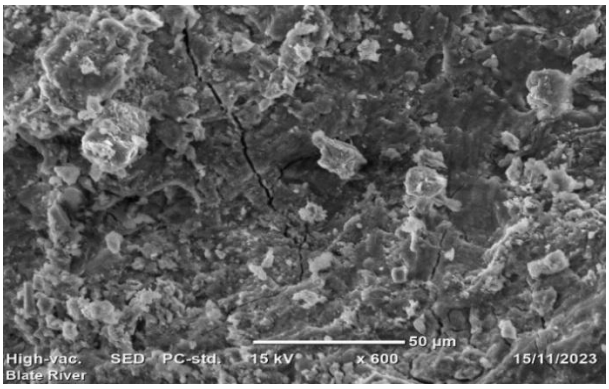

Figure 14. SEM Blate River sand 28th day Concrete

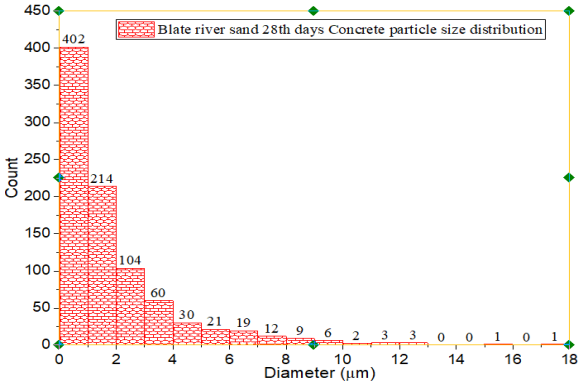

Figure 15. Blate River sand 28th day Concrete PSD

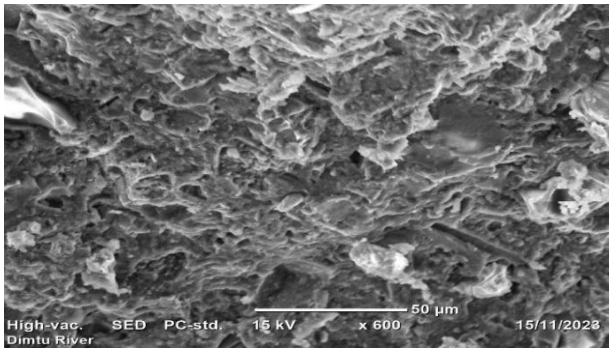

Figure 16. SEM Dimtu River sand 28th day Concrete

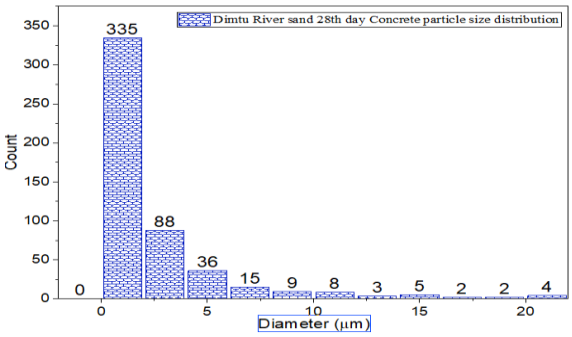

Figure 17. Dimtu River sand 28th day PSD

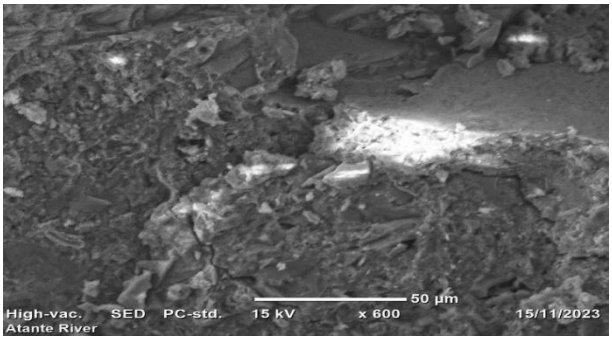

Figure 18. SEM Hantate River sand 28th day Concrete

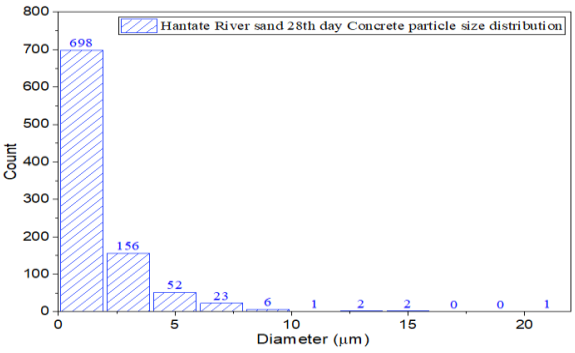

Figure 19. Hantate River sand 28th day Concrete PSD

The Langano Quarry sand concrete displays distinct, angular, and blocky particles (Figure 20), typical of crushed aggregate, and has the lowest ultrafine content (233 counts, Figure 21) with more particles in the intermediate size ranges, implying superior mechanical interlock and a coarser material structure.

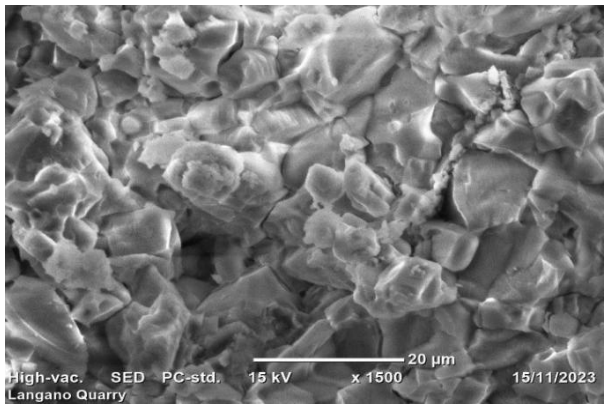

Figure 20. SEM Langano quarry sand 28th day Concrete

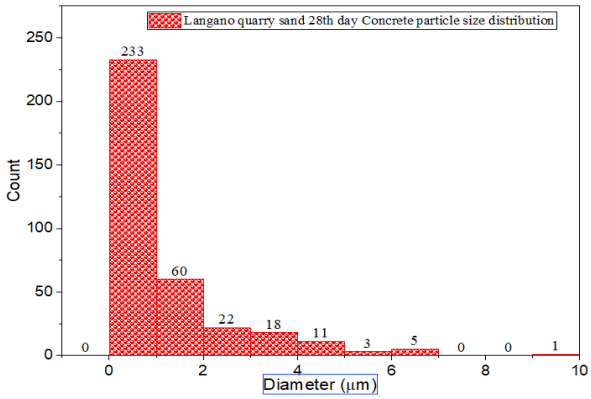

Figure 21. Langano quarry sand 28th day Concrete PSD

The Shamena Quarry sand concrete shows a closely packed, fine-grained texture (Figure 22) and the best-graded particle distribution (Figure 23), with 374 ultrafine counts followed by a gradual decrease across subsequent sizes, which often leads to optimal packing density

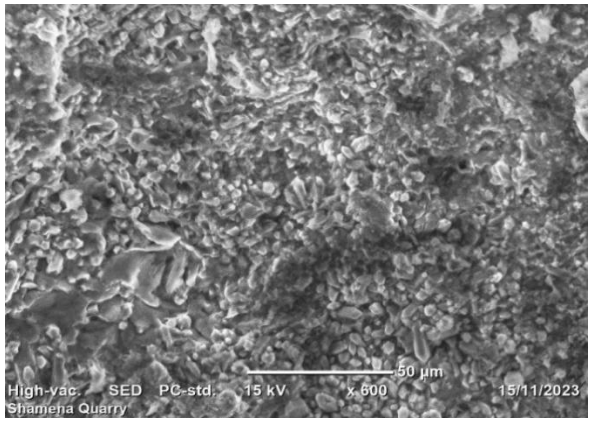

Figure 22. SEM Shamena quarry sand 28th day Concrete

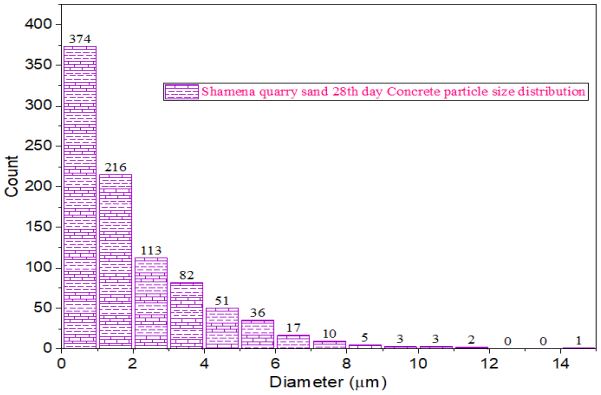

Figure 23. Shamena quarry sand 28th day Concrete PSD

The Weterarasa River sand concrete shows a smooth matrix and a skewed particle distribution, heavily concentrated in the 0-2 µm range, indicating potential grading deficiencies and increased shrinkage risks.

The SEM observations indicated that there were strong variations in densification of the matrix, pore distribution and quality of the ITZ of the mixes of concrete. The concretes manufactured using Dimtu River sands and Hantate River sands had compact microstructure and microcracking that was not very extensive and had hydrated products that had developed well. Conversely, concretes with Ayermarefiya and Shamena quarry sands showed porous matrices with obvious voids and micro-cracks, which is evidence of poor packing of particles and inefficient hydration.

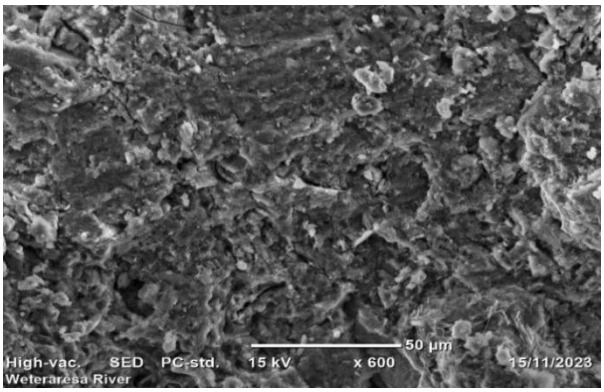

Figure 24. SEM Weteraresa River sand 28th day Concrete

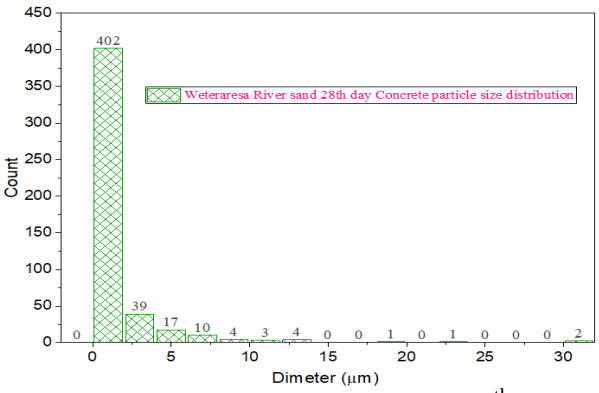

Figure 25. Weteraresa River sand 28th day Concrete PSD

The quantitative porosity analysis proved the existence of an inverse relationship between the area of pores and compressive strength. Blends with a higher proportion of pore areas continued to have lower strength, and it supports the conclusion that microstructural compactness dominate the mechanical performance of the blends (Figure 26). The findings can be supported by previous research that porosity is one of the main controlling parameters of concrete strength and durability (Bentz et al., 2017).

The porosity results show variation among concrete mixes made with different river and quarry sand sources. Mixes with lower porosity generally exhibited higher compressive strength due to a denser cement matrix, while mixes with higher porosity showed lower strength because increased void spaces weaken the internal structure of the concrete.

Table 5. Area of pores in natural sand and 28th days Concrete

Combination ID	**Area of Pores (%)**	
	Natural Sand	**28th Days Concrete**
Aje (Bura)Quarry	14.032	23.857
Ayermarefiya Quary	20.688	25.639
Blate River	10.325	23.404
Dimitu River	10.17	28.564
Hantate River	10.396	18.68
Langano Quarry	20.07	23.636
Shamena Quarry	19.87	22.806
Weteraresa River	13.938	17.959
Coarse Aggregate	**27.359**	

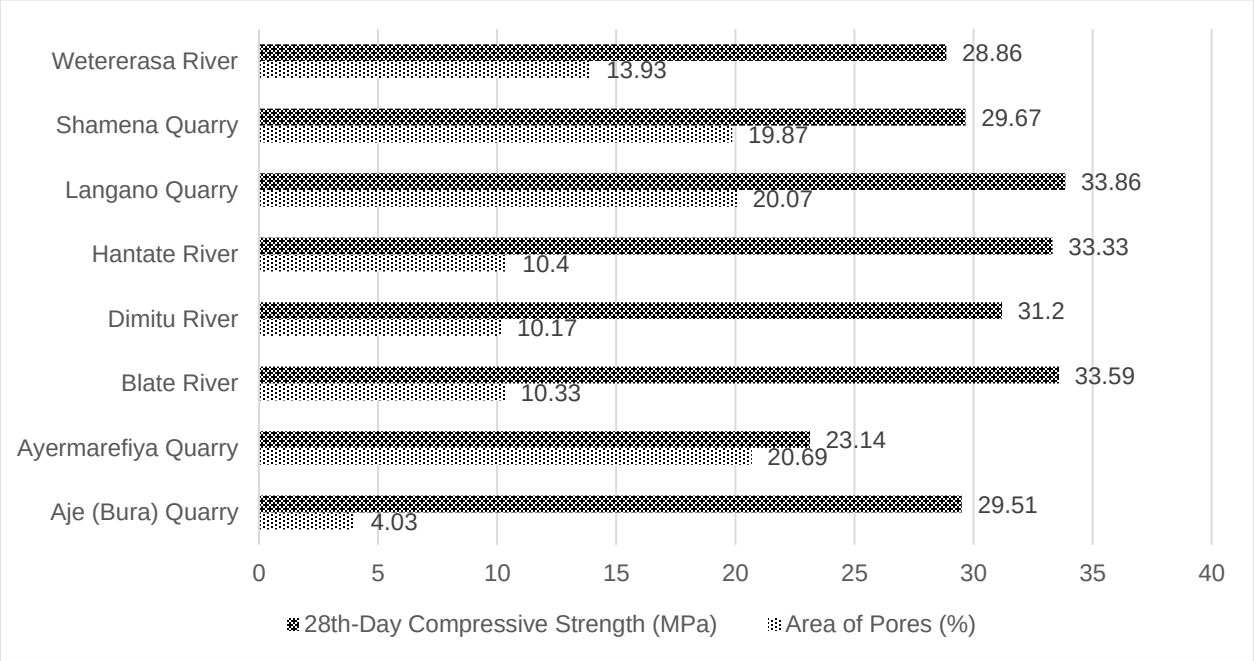

Figure 26. Comparison of compressive strength and porosity

3.7. Integrated Performance Assessment

After the synthesis of mechanical and microstructural findings, the suitability of the sand sources to structural concrete can be ordered in decreasing order of their performances as follows: Hantate River, Langano Quarry, Blate River, Dimtu River, Aje (Bura) Quarry, Weteraresa River, Shamena Quarry and Ayermarefiya Quarry. Sands that were lower in this order had too many fines, were absorptive and had a poor mineralogical makeup that together had a negative and negative effect on the performance of concrete. These results indicate that quarry sand cannot be absolutely excluded in the structural performances; instead, its appropriateness has to be determined in accordance with strict physicochemical and microstructural examination. Effective processing, washing and grading of quarry sand can contribute greatly to its performance in a way favorable to the sustainable use of aggregates without compromising the structural integrity of the sand.

4. Conclusion

This research paper has provided an extensive analysis of the mechanical and microstructural performance of the concrete made of river and quarry sands that are obtained in various sites in the surroundings of Hawassa City, Ethiopia. The findings indicate that the variance in source of sand has a significant effect on the performance of concrete because there were significant differences in physical, chemical, and mineralogical aspects resulting in significant differences in compressive strength and tensile strength, water absorption, and microstructural compactness. In terms of mechanical performance and microstructure density, concrete built with Hantate River sand consistently outperformed concrete made using quarry sands. The exception hinged on

quality, though, since well-processed quarry sand—particularly Langano—performed similarly because these materials are beneficial in structural concrete when the necessary quality standards are met.

The study also discovered that the primary causes of strength loss are organic contaminants, high water absorption, and excessive fines. Concrete made from sands with a high silt and clay content and a low specific gravity, such as those from Ayermarefiya and Shamena, had a larger porosity, fewer interfacial transition zones, and lower compressive and tensile strengths. The results of the SEM demonstrated that dense microstructures and well-developed hydration products increase strength and decrease permeability, and the microstructural analysis demonstrated that the densification of matrices and the distribution of pores affect mechanical behavior. Quartz was the predominant mineral phase, according to XRD analysis, and the crystallinity varied to affect the hydration performance and longevity.A negative correlation existed between the pore area and compressive strength, which indicated porosity as a performance-controlling factor in all mixes of concrete.

Funding

No Funding has been received.

Competing Interests

The authors declare no competing interests.

Concerns to Publish

All the authors concern to the publication of this article.

Reference

AASHTO. (2019a). AASHTO T96: Standard Method of Test for Resistance to Degradation of Small-Size Coarse Aggregate by Abrasion and Impact in the Los Angeles Machine.

AASHTO. (2019b). AASHTO T104: Standard Method of Test for Soundness of Aggregate by Use of Sodium Sulfate or Magnesium Sulfate.

Ali, M., Qureshi, L. A., & Raza, A. (2023). Performance evaluation of quarry sand as a partial replacement of river sand in concrete. Construction and Building Materials, 366, 130210. https://doi.org/10.1016/j.conbuildmat.2023.130210

American Concrete Institute (ACI). (2009). ACI 211.1: Standard Practice for Selecting Proportions for Normal, Heavyweight, and Mass Concrete.

Aslani, F., Kelin, J., & Ma, G. (2020). Mechanical and durability properties of concrete containing manufactured sand. Journal of Materials in Civil Engineering, 32(6), 04020123. https://doi.org/10.1061/(ASCE)MT.1943-5533.0003147

ASTM International. (2014). ASTM D75/D75M: Standard Practice for Sampling Aggregates.

ASTM International. (2018). ASTM C29/C29M: Standard Test Method for Bulk Density (Unit Weight) and Voids in Aggregate.

ASTM International. (2020a). ASTM C127: Standard Test Method for Relative Density (Specific Gravity) and Absorption of Coarse Aggregate.

ASTM International. (2020b). ASTM C128: Standard Test Method for Relative Density (Specific Gravity) and Absorption of Fine Aggregate.

ASTM International. (2021a). ASTM C88/C88M: Standard Test Method for Soundness of Aggregates by Use of Sodium Sulfate or Magnesium Sulfate.

ASTM International. (2021b). ASTM C1602/C1602M: Standard Specification for Mixing Water Used in the Production of Hydraulic Cement Concrete. Publisher: ASTM International.

ASTM International. (2022a). ASTM C40/C40M: Standard Test Method for Organic Impurities in Fine Aggregates for Concrete.

ASTM International. (2022b). ASTM C143/C143M: Standard Test Method for Slump of Hydraulic-Cement Concrete.

ASTM International. (2022c). ASTM C150/C150M-22: Standard Specification for Portland Cement. https://www.astm.org/c0150_c0150m-22.html

ASTM International. (2022d). ASTM C805/C805M: Standard Test Method for Rebound Number of Hardened Concrete.

ASTM International. (2023a). ASTM C33/C33M: Standard Specification for Concrete Aggregates.

ASTM International. (2023b). ASTM C403/C403M-23: Standard Test Method for Time of Setting of Concrete Mixtures by Penetration Resistance.

ASTM International. (2023c). ASTM C566: Standard Test Method for Total Evaporable Moisture Content of Aggregate by Drying.

Bentz, D. P., Arnold, J., Boisclair, M. J., Jones, S. Z., Rothfeld, P., Stutzman, P. E., Tanesi, J., Beyene, M., Kim, H., Munoz, J., & Ardani, A. (2017). Influence of aggregate characteristics on concrete performance. NIST. https://doi.org/10.6028/NIST.TN.1963

Bragg, W. H., & Bragg, W. L. (1913). The reflection of X-rays by crystals. Proceedings of the Royal Society A, 88(605), 428–438. https://doi.org/10.1098/rspa.1913.0040

British Standards Institution. (1990). BS 812-110: Testing aggregates—Methods for determination of aggregate crushing value (ACV).

Domagała, L. (2015). The Effect of Lightweight Aggregate Water Absorption on the Reduction of Water-Cement Ratio in Fresh Concrete. Procedia Engineering, 108, 206–213. https://doi.org/10.1016/j.proeng.2015.06.139

Elat, E., Pliya, P., Pierre, A., Mbessa, M., & Noumowé, A. (2020). Microstructure and Mechanical Behavior of Concrete Based on Crushed Sand Combined with Alluvial Sand. CivilEng, 1(3), 181–197. https://doi.org/10.3390/CIVILENG1030011

Ethiopian Standards Agency. (2012). ES C.D6:2012 (OPC 42.5N).

IS. (1963a). IS 2386 (Part I): Methods of Test for Aggregates for Concrete—Particle Size and Shape.

IS. (1963b). IS 2386 (Part IV): Methods of Test for Aggregates for Concrete—Mechanical Properties.

Kebede, A., Taffesse, W., & Gebrehiwot, K. (2022). Evaluation of concrete properties using locally available sands in Ethiopia. Materials Today: Proceedings, 62, 4871–4878. https://doi.org/10.1016/j.matpr.2022.03.212

Kumar, R., & Ransinchung, G. D. (2023). Sustainability assessment of alternative fine aggregates in concrete. Resources, Conservation and Recycling, 188, 106711. https://doi.org/10.1016/j.resconrec.2022.106711

Mehta, P. K., & Monteiro, P. J. M. (2014). Concrete: Microstructure, Properties, and Materials (4th ed.). McGraw-Hill Education.

Neville, A. M. (2011). Properties of Concrete (5th ed.). Pearson Education.

Raja, R., & Vijayan, P. (2020). Strength and Microstructural Behaviour of Concrete Incorporating Laterite Sand in Binary Blended Cement. Revista de La Construccion, 19(3), 422–430. https://doi.org/10.7764/RDLC.19.3.422

Scherrer, P. (1918). Bestimmung der Größe und der inneren Struktur von Kolloidteilchen mittels Röntgenstrahlen. Nachrichten von Der Gesellschaft Der Wissenschaften Zu Göttingen, Mathematisch-Physikalische Klasse, 1918, 98–100.

Siddique, R., & Singh, M. (2022). Utilization of quarry dust in concrete: A review. Journal of Cleaner Production, 341, 130842. https://doi.org/10.1016/j.jclepro.2022.130842

Singh, P., Patel, A., & Sharma, R. (2024). Effect of aggregate morphology on microstructural behavior of concrete. Construction and Building Materials, 392, 131997. https://doi.org/10.1016/j.conbuildmat.2024.131997

Zhao, Y., Li, J., & Wang, X. (2023). Microstructural characterization of concrete using SEM and XRD techniques. Cement and Concrete Research, 165, 107015. https://doi.org/10.1016/j.cemconres.2023.107015